Electronic Supplementary Information

Effects of Water Vapor and Oxygen on Non-Fullerene Small Molecule Acceptors

Chuanfei Wang,[*a] *Shaofei Ni,*[b] *Slawomir Braun,*[a] *Mats Fahlman,*[*a] *Xianjie Liu*[a]

[a]Division of Surface Physics and Chemistry, IFM, Linköping University, SE-58183, Linköping, Sweden.

[b]Institute of Chemical Research of Catalonia, Tarragona, 43007 Spain

Email: chuanfei.wang@liu.se, mats.fahlman@liu.se

Contents

Experiment Methods

Photoelectron spectroscopy

The thin films (≈20 nm) were spin-coated onto AlO_x/Al (Al) from 5 mg/mL o-dichlorobenzene solutions under nitrogen atmosphere in dark condition, then directly and quickly (≈4 min) transferred using a container covered with aluminum foil to shield from illumination, into the load lock chamber of the ultrahigh vacuum (UHV) system used for the experiments. All substrates were cleaned by sonication in isopropyl alcohol before spin coating. The photoemission experiments were done in an UHV surface analysis system, consisting of an entry chamber (base pressure ≈1 × 10^{-7} mbar), a preparation chamber (≈8 × 10^{-10} mbar), and an analysis chamber (≈2 × 10^{-10} mbar). In situ exposure of *o*-IDTBR and *p/ m*-ITIC film to oxygen and water vapor respectively was carried out in the preparation chamber under the pressure of 6.5 × 10^{-6} mbar controlled via a leak- valve. After each exposure step, the film samples were transferred to the analysis chamber without breaking UHV for measurements. UPS (HeI hν = 21.22 eV) and XPS (monochromatized AlKα hν = 1486.6 eV) spectra were recorded with a Scienta-200 hemispherical analyzer and calibrated by referencing to Fermi level and Au 4f 7/2 peak position of the Ar + ion sputter-clean gold foil. UPS was performed to study the interfacial alignment and the frontier electronic structure features with an error margin of ±0.05 eV. The work function is derived from the secondary electron cut-off and the vertical IP from the frontier edge of the occupied density of states. XPS was used to detect possible chemical reaction and element absorption in the films after exposure. All water/ O_2 exposure and measurements were carried out in chambers shielded from UV light (by aluminum foil) and under near-dark conditions (ambient UHV chamber light). The samples were shielded from UV light during O_2 /water vapor exposure as OPV cells likely will be manufactured on glass or plastic (e.g., poly (ethylene terephthalate), PET) substrates, the latter typically featuring UV-absorbers/blockers as PET itself photo degrades due to UV light.

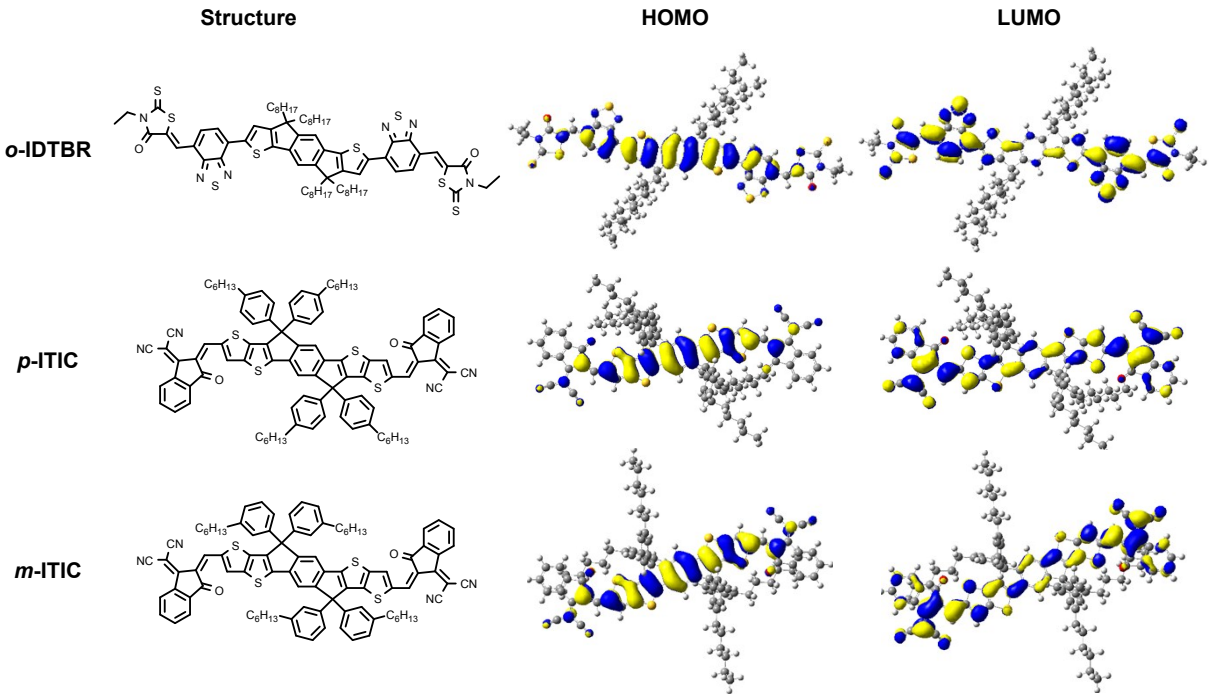

Fig. S1. Chemical structure and frontier energy level distribution of *o*-IDTBR, *p*-ITIC and *m*-ITIC.

Table S1. Energy levels of *o*-IDTBR, *p*-ITIC and *m*-ITIC.

	IP[a] (eV)	EA[b] (eV)	E_{ICT}[c] (eV)	Eg opt[d]. (eV)
$PC_{71}BM$	5.90±0.1	4.18	4.35±0.05	1.72
o-IDTBR	5.54±0.1	3.82	3.94±0.05	1.72[e]
p-ITIC	5.63±0.1	4.01	4.19±0.05	1.62
m-ITIC	5.64±0.1	4.02	4.20±0.05	1.62

[a] Measured by UPS. [b]Calculated from IP and optical gap. [c]Deduced from the UPS. [d]Estimated from the onset of the absorption spectra. [e]Estimated from absorption onset of o-IDTBR $CHCl_3$ solution.

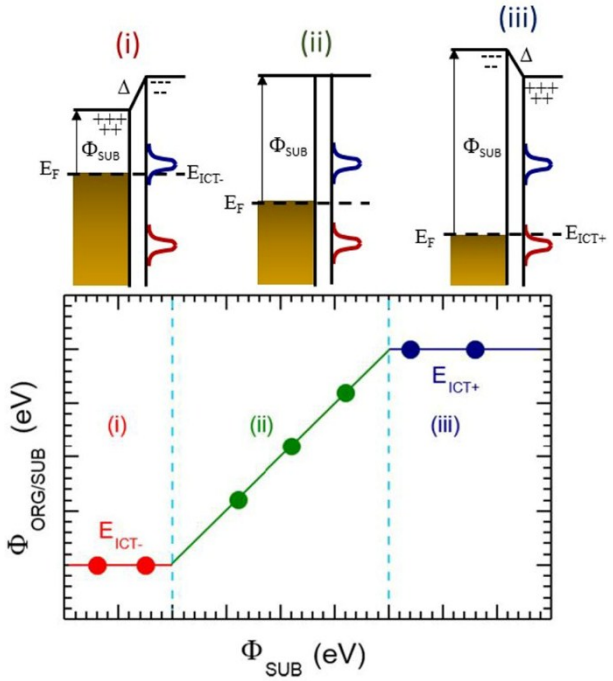

Fig. S2. Integer charge transfer (ICT) model.
ⅰ) Fermi level is pinned to negative integer charge transfer state. ⅱ) Valcumm level aligment region betweeen substrate and organic thin film. ⅲ) Fermi level is pinned to positive integer charge transfer state.

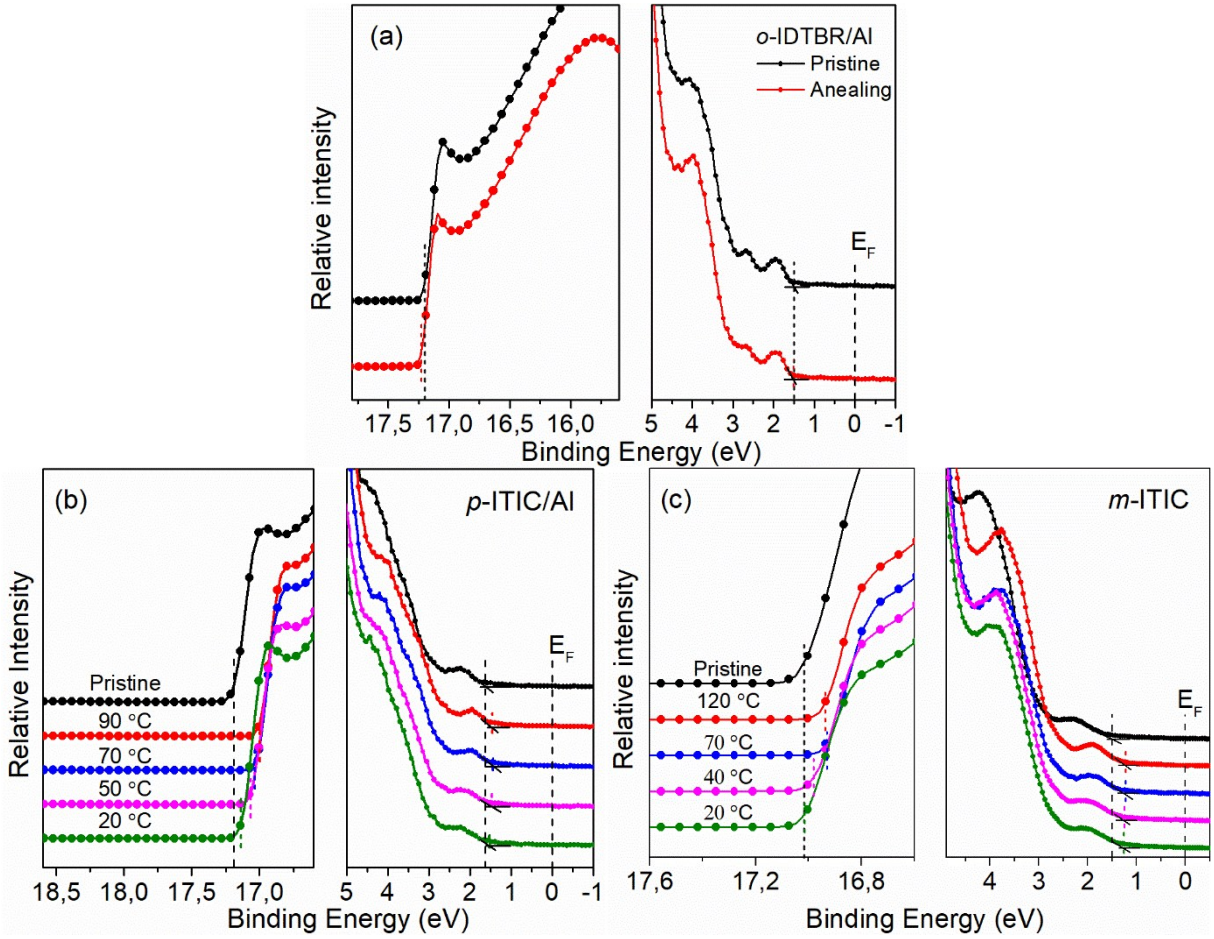

Fig. S3. Thermal annealing treatment of a) *o*-IDTBR, b) *p*-ITIC and c) *m*-ITIC.

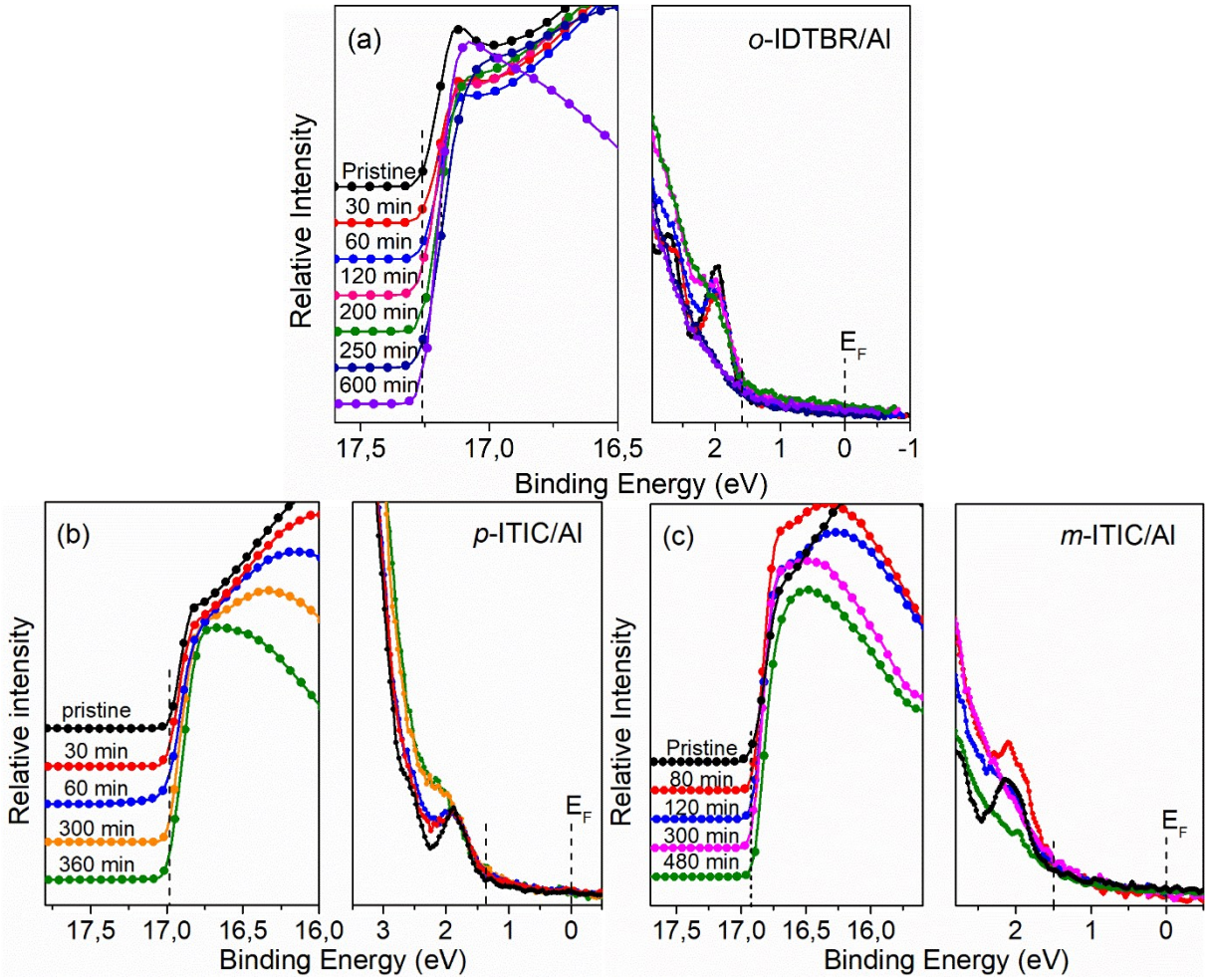

Fig. S4. UPS spectra evolution under in situ oxygen exposure a) a) *o*-IDTBR, b) *p*-ITIC and c) *m*-ITIC. All the spectrums are aligned at high binding energy.

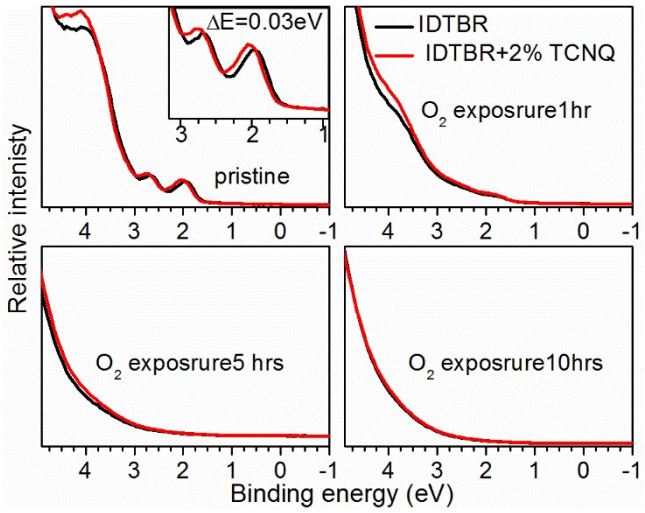

Fig. S5. Effect of TCNQ on the oxygen exposure degradation.

Table S2. Comparison of energy level between pristine and oxygen attached molecules.

	o-IDTBR	*o*-IDTBR·····O_2	*o*-IDTBR·····$2O_2$	*o*-IDTBR·····$3O_2$
LUMO (eV)	-2.511	-2.690[a] -2.703[b]	-2.726[ab] -2.712[a*b] -2.690[bb] -2.702[bb*]	-2.730[bab] -2.739[ba*b] -2.712[bab*]
Difference (eV)	0.000	-0.179 -0.192	-0.215 -0.201 -0.179 -0.191	-0.219 -0.228 -0.201
HOMO	-6.395	-6.432[a] -6.490[b]	-6.526[ab] -6.473[ba*] -6.476 [bb] -6.525[bb*]	-6.567[bab] -6.568 [ba*b] -6.576 [bab*]
Difference (eV)	0.000	-0.095 -0.037	-0.131 -0.078 -0.081 -0.130	-0.172 -0.173 -0.181
	p-ITIC	*p*-ITIC·····O_2	*p*-ITIC·····$2O_2$	*p*-ITIC·····$3O_2$
LUMO (eV)	-2.847	-2.851[a] -2.894[b]	-2.865[ab] -2.910[bb]	-2.925[bab]
Difference (eV)	0.000	-0.004 -0.047	-0.018 -0.063	-0.078
HOMO (eV)	-6.680	-6.734[a] -6.691[b]	-6.618[ab] -6.700[bb]	-6.754[bab]
Difference (eV)	0.000	-0.054 -0.011	+0.062 -0.020	-0.074
	m-ITIC	*m*-ITIC·····O_2	*m*-ITIC·····$2O_2$	*m*-ITIC·····$3O_2$
LUMO (eV)	-2.895	-2.897[a] -2.930[b]	-2.963[ab] -2.973[bb]	-2.971[bab]
Difference (eV)	0.000	-0.002 -0.035	-0.068 -0.078	-0.076
HOMO (eV)	-6.716	-6.775[a] -6.742[b]	-6.787[ab] -6.745[bb]	-6.795[bab]
Difference (eV)	0.000	-0.059 -0.026	-0.071 -0.029	-0.079

[a]represent middle location, [b]represent terminal loction and *represent different side of the plane. Example can be found in Fig. S6

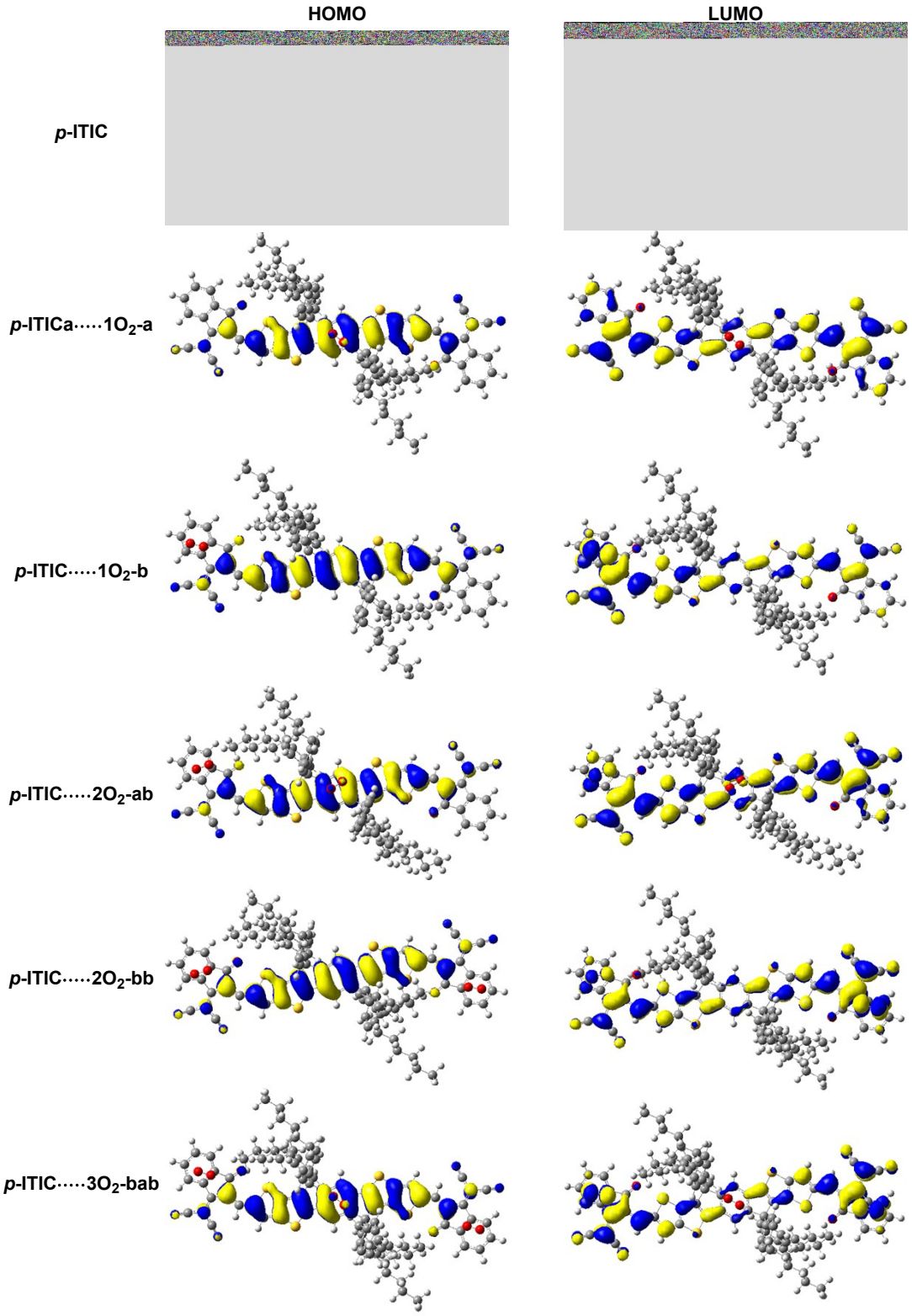

Fig. S6. Frontier molecular orbitals distribution of *p*-ITIC and O_2·····*p*-ITIC.

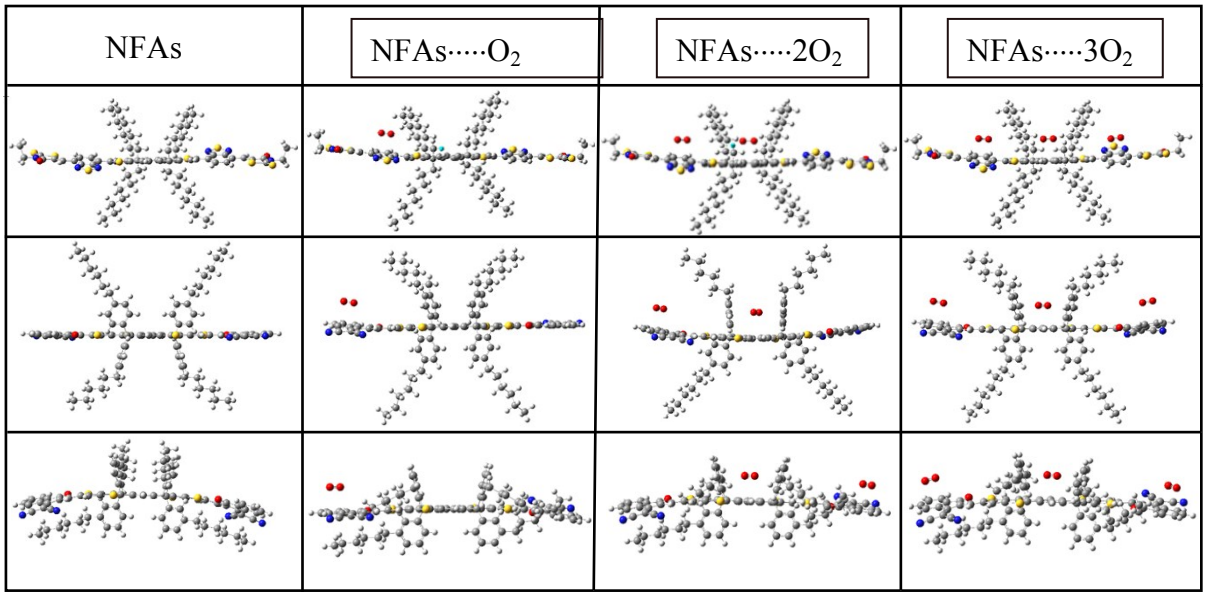

Fig. S7. The calculated molecular structures of *o*-IDTBR, *p*-ITIC and *m*-ITIC from top to bottom.

Table S3. The calculated dihedral of *o*-IDTBR, *p*-ITIC and *m*-ITIC.

	NFAs	NFAs·····O_2	NFAs·····$2O_2$	NFAs·····$3O_2$
o-IDTBR	19.15	19.78	20.72	20.71
p-ITIC	1.27	3.44	3.17	3.61
m-ITIC	9.48	3.25	4.41	9.17

The geometric structures of all species were optimized by the M06-2X functional in Gaussian 09 program.[1] The all-electron basis set 6-311G** was used in describing all the atoms. The oxygen molecule has been considered in its stable triplet ground state, and a UM06-2X/6-311G** calculation has been carried out. Different kinds of interactions between the moleculars and O_2 by varying the positions and numbers of dioxygen have been considered and totally 19 interaction models have been tested in our calculations.

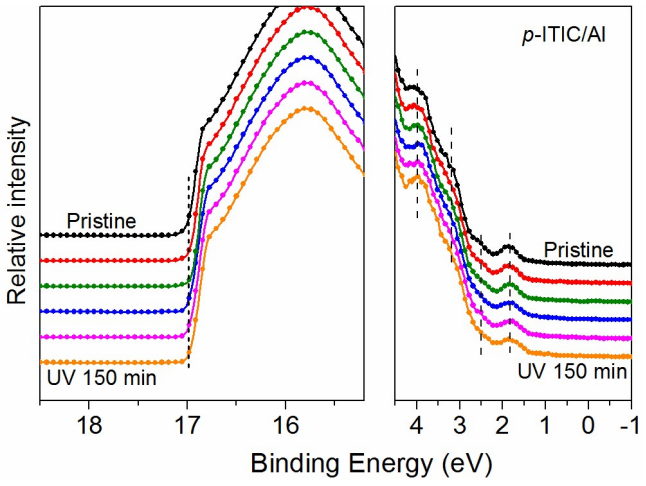

Fig. S8. UV-light illumination on *p*-ITIC.

The acceptor *p*-ITIC was exposed to UV-light. As shown in **Fig. S8**. The HOMO properties show little change compared to pristine film after 2.5 hours UV-light illumination under UHV chamber within the measurement error bar, indicating the tolerance of non-fullerene acceptor *p*-ITIC to UV-light illumination without attendance of the water vapor and oxygen.

References

[1] M. J. Frisch, G. W. Trucks, H. B. Schlegel, G. E. Scuseria, M. A. Robb, J. R. Cheeseman, G. Scalmani, V. Barone, B. Mennucci, G. A. Petersson, H. Nakatsuji, M. Caricato, X. Li, H. P. Ratchian, A. F. Izmaylov, J. Bloino, G. Zheng, J. L. Sonnenberg, M. E. Hada, M., K. F. Toyota, R., J. Hasegawa, M. Ishida, T. Nakajima, Y. Honda, O. N. Kitao, H., T. Vreven, J. A. Montgomery, Jr., J. E. Peralta, F. Ogliaro, M. Bearpark, J. J. Heyd, E. Brothers, K. N. Kudin, V. N. Staroverov, T. Keith, R. Kobayashi, J. Normand, K. Raghavachari, A. Rendell, J. C. Burant, S. S. Iyengar, J. Tomasi, M. Cossi, N. Rega, J. M. Millam, M. Klene, J. E. Knox, J. B. Cross, V. Bakken, C. Adamo, J. Jaramillo, R. Gomperts, R. E. Stratmann, O. Yazyev, A. J. Austin, R. Cammi, C. Pomelli, J. W. Ochterski, R. L. Martin, K. Morokuma, V. G. Zakrzewski, G. A. Voth, P. Salvador, J. J. Dannenberg, S. Dapprich, A. D. Daniels, O. Farkas, J. B. Foresman, J. V. Ortiz, J. Cioslowski, D. J. Fox, Gaussian 09, Revision D.01, Wallingford CT (2013).